REEXAMINATION OF PROTON-INDUCED REACTIONS ON $^{\rm nat}{\rm Mo}$ AT 19–26 MeV AND STUDY OF TARGET YIELD OF RESULTANT RADIONUCLIDES

Arshiya A. Ahmed[†], A. Wrońska[‡], A. Magiera

M. Smoluchowski Institute of Physics, Jagiellonian University Łojasiewicza 11, 30-348 Kraków, Poland

M. Bartyzel, J.W. Mietelski, R. Misiak, B. Was

H. Niewodniczański Institute of Nuclear Physics Polish Academy of Sciences Radzikowskiego 152, 31-342 Kraków, Poland

(Received September 9, 2019; accepted October 31, 2019)

As an alternative to reactor-based $^{99}\text{Mo}/^{99m}\text{Tc}$ generator technology, many research groups have suggested the direct production of ^{99m}Tc on highly enriched ^{100}Mo through accelerators. For proton-induced reaction, there is a large discrepancy in 9–26 MeV beam energy range in the data available for the production of radionuclides impurities. In this work, we studied target yield and the cross section for the production of long-lived radionuclides produced in the $^{\text{nat}}\text{Mo}$ target irradiated with a proton beam of energy degraded from 26 to 19 MeV in the target. This constitutes the first step, which is a commissioning of the setup and a check of the method at the beam energy where cross sections of interest are large. The step was necessary before proceeding with more demanding measurements at lower energies. Target yield was derived using the measured activity of produced radionuclides. Total cross sections for all isotopes produced from $^{\text{nat}}\text{Mo}(p,x)$ reactions are presented and compared with the previously available data, showing good agreement.

DOI:10.5506/APhysPolB.50.1583

1. Introduction

About 80% of diagnostic imaging techniques in nuclear medicine involve technetium-99 at meta-stable state (99m Tc) radioisotope. Around 2011, the failure of two major reactors involved in the production of 99 Mo, which is the

[†] arshiya.anees.ahmed@doctoral.uj.edu.pl

[‡] aleksandra.wronska@uj.edu.pl

generator of 99m Tc, made the nuclear physics community realize the upcoming shortfall in the production of these isotopes [1]. Soon afterwards, new production paths were proposed in the literature [2–5], exploiting proton beam accelerated in cyclotrons: through (p, 2n) reaction on highly enriched ¹⁰⁰Mo. It is still possible to produce ⁹⁹Mo and ^{99m}Tc by proton-induced reaction on natural molybdenum (nat Mo). Using natural target will be advantageous if activity of other radioisotopes is sufficiently small. Molybdenum is also used in accelerator applications as corrosion resistant and refractory metal, thus it is important to study proton-induced reaction cross section at the intermediate energy range. A quite substantial database is available for cross section of proton-induced reactions on both ^{nat}Mo and enriched ¹⁰⁰Mo [2, 3, 6–19], but there are large discrepancies between individual data sets. Besides, there is insufficient experimental data available for the impurities produced along with the ⁹⁹Mo/^{99m}Tc [20]. In all the previously reported data the shape of the excitation curve is generally similar, but they differ in magnitude by a factor of 2. Hence, in the present work, we measured the production cross sections of ⁹⁹Mo, ^{99m}Tc (direct production) and other longlived radioisotope impurities produced in proton-induced reaction on natural molybdenum by standard single-target activation technique at 19–26 MeV energy range. We also determined directly from our experimental data the integral target yield in this energy range for all the radioisotopes produced in ^{nat}Mo which could be identified in the gamma spectrum. In [16], authors have provided the recommended cross-section data for gamma emitting diagnostic radioisotopes using previously published data and new experimental data which is helpful in validating the produced data.

2. Experiment

2.1. Beam, target and irradiation procedure

The target used in the experiment was natural molybdenum with the following isotopic composition: $^{92}\mathrm{Mo}$ 14.64%, $^{94}\mathrm{Mo}$ 9.18%, $^{95}\mathrm{Mo}$ 15.87%, $^{96}\mathrm{Mo}$ 16.67%, $^{97}\mathrm{Mo}$ 9.58%, $^{98}\mathrm{Mo}$ 24.29%, and $^{100}\mathrm{Mo}$ 9.74% [21], in the form of a metallic disc (25 mm in diameter, 0.5 mm thick and 99.9% pure) purchased from Goodfellow Cambridge Limited, UK. The thickness of the target was verified by weighing the target on the micro-balance and measuring the target's surface.

The irradiation was done at an external beam line of AIC-144 cyclotron in the Institute of Nuclear Physics Polish Academy of Sciences, Kraków, Poland. It is an isochronous cyclotron which is capable of accelerating protons in the form of a collimated beam with energy of 60 MeV and intensity of 65 nA. Since the cyclotron produces mono-energetic protons and beam energy cannot be varied, we used 99% pure aluminum foils (11.7 mm thick)

as degraders. The average beam energy at the exit of the degrader was calculated using SRIM [22] and Geant4 simulation software [23], and was found to be 26 MeV and the value energy straggling was 0.16 MeV. The target was irradiated for 5 hours. After the end of bombardment (EOB), the target was left to cool down for 18 hours (cooling time $t_{\rm c}=18~{\rm h}$).

Gamma-ray attenuation and the beam spread was studied using Geant4 simulations. Gamma attenuation within the target was about 0.5% (on average). The dimension of the proton beam was measured using a fluorescent sheet at the position of the Al degrader. The diameter of the beam was 5 mm. Then the degrader beam size was 2 cm in diameter and at the exit of the target, the beam was 2.3 cm which is less than the diameter of the target. Hence, the entire beam was incident on the target.

2.2. Radioactivity measurement

The measurements of activity (gamma-ray counting) were done using an energy and efficiency calibrated HPGe detector. The energy and efficiency calibration of the detector was performed using a set of standard sources (133 Ba, 60 Co, 152 Eu, 22 Na, and 137 Cs) for the sample-detector distance of 52 cm. The detector efficiency ϵ was described as follows:

$$\ln(\epsilon) = \sum_{n=0}^{4} a_n (\ln E)^n, \qquad (1)$$

where E [keV] is the gamma energy and a_n are fitted coefficients. The sample was measured at the same distance as used for efficiency calibration.

The first registered spectrum is shown in Fig. 1. The list of identified in this study radionuclides is presented in Table I. The data for half-lives, gamma-ray energies and intensities of transitions in radionuclides were adopted from the Nuclear Data Service, IAEA [24].

2.3. Interference process corrections and cross-section determination

As is discussed in [14, 15, 17, 18], many radionuclides produce gamma lines of the same or nearly the same energy. For example, radioisomers 94 Tc and 94m Tc decay produce 871.09 keV gamma quanta. The isotopes decaying to the same product also emit gamma of the same energy 94 Tc $^{-94}$ Nb, 95 Tc $^{-95}$ Nb, and 96 Tc $^{-96}$ Nb. The most complicated case in our analysis is the 140.51 keV spectral line (90 Nb, 99 Mo, 99m Tc).

To determine the cross section of 99m Tc direct production, one needs to use an intense beam for a short irradiation time and a short cooling period. For accurate estimation, both irradiation and cooling time should be shorter than $\frac{1}{10}$ of the half-life of 99m Tc [15]. One can then use the

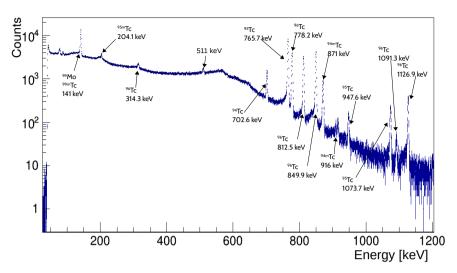


Fig. 1. Gamma spectrum of ^{nat}Mo target irradiated with a 26 MeV and 28.5 nA proton beam for five hours, recorded after 18 hours of cooling time.

standard activation formula (2) to find the direct production cross section of 99m Tc. If the above-mentioned conditions are not met, one needs to add appropriate corrections to the measured gamma yields or modify the standard activation formula [18]. In the calculations, we have neglected the contribution of 90 Nb, since the nat Mo $(p,x)^{90}$ Nb reaction cross section at 19–26 MeV is negligible [25]. Then the dependence of the activity for 99 Mo is described by the standard activation formula (2) and for 99m Tc, the modified formula (3) is used

$$A(t) = n_0 I \sigma \left(1 - e^{-\lambda t_{\rm irr}} \right) e^{-\lambda t} , \qquad (2)$$

$$A_{\rm Tcm}(t) = n_0 I \left[\left(\sigma_{\rm Tcm} + P_{\rm Mo} \frac{\lambda_{\rm Mo}}{\lambda_{\rm Mo} - \lambda_{\rm Tcm}} \sigma_{\rm Mo} \right) \times \left(1 - e^{-\lambda_{\rm Tcm} t_{\rm irr}} \right) e^{-\lambda_{\rm Tcm} t} - P_{\rm Mo} \frac{\lambda_{\rm Tcm}}{\lambda_{\rm Mo} - \lambda_{\rm Tcm}} \times \sigma_{\rm Mo} \left(1 - e^{-\lambda_{\rm Mo} t_{\rm irr}} \right) e^{-\lambda_{\rm Mo} t} \right] , \qquad (3)$$

where subscripts Mo, Tcm refer to 99 Mo and 99m Tc isotopes, A is the activity of the isotope at time t, λ is the decay constant, I is beam current expressed as a number of incident particles per second, n_0 is the surface density of the target, σ is reaction cross section. P_{Mo} is the decay fraction of 99 Mo to 99m Tc which is 0.876, and t_{irr} refers to irradiation time.

TABLE I

Nuclear data for Tc and Mo radionuclides produced at 19–26 MeV proton on ^{nat}Mo target. Gamma energies used in this study are in bold. Uncertainties of the half-life, gamma energies and the corresponding intensities in the last valid digits are in italics.

Radionuclides	Half life $(T_{1/2})$		E_{γ} [keV]		I_{γ} [%]	
⁹⁴ Tc	293 min	1	702.622 849.74 871.091	19 7 18	99.6 95.7 99.9	18 18
$^{94m}{ m Tc}$	52.0 min	10	871.091 993.19 1522.11 1868.68	18 9 20 8	94 2.21 4.5 5.7	3 3 3
$^{95}{ m Tc}$	20.0 h	1	765.794 947.67 1073.71	7 2 2	93.82 1.951 3.74	19 19 4
$^{95m}\mathrm{Tc}$	61 d	2	204.117 582.082 835.149	2 3 5	63.25 29.96 26.63	13 5 19
⁹⁶ Tc	4.28 d	7	314.337 778.224 812.581 849.929 1126.965	71 15 15 13 21	2.43 99.9 82 98 15.2	24 4 4 12
⁹⁹ mTc ⁹⁹ Mo	6.01 h 65.94 h	1 1	140.511 140.511 181.063 739.50	1 1 8 2	89 89.43 5.99 12.13	23 7 12

As we can see from Eq. (3), activity of 99m Tc is the sum of two exponential components, one with decay constant of 99m Tc and the other of 99 Mo, because during irradiation 99m Tc can be produced directly in the reaction nat Mo $(p,x)^{99m}$ Tc and through decay of 99 Mo. To calculate the cross section for 99m Tc production deduced from the 140.51 keV photo peak, Eq. (3) is used and all other cross-section calculations are done using the standard activation formula.

2.4. Target yield (TY)

For the known cross section, the target yield (TY) is calculated using Eq. (4), in which decay during the irradiation time is taken into account

$$TY_{\sigma} = \frac{HN_{A}\lambda}{Mze} \int_{E_{min}}^{E_{max}} \frac{\sigma(E)}{S(E)} dE, \qquad (4)$$

where H is isotopic enrichment of the target, $N_{\rm A}$ is Avogadro's number, M is atomic mass of the target, z is atomic number of the incident particle, e is electron charge, S is the stopping power of the incident particle in the target, E is the energy of the projectile, $E_{\rm max}$ is the maximum energy of the incident particle when it hits the target, and $E_{\rm min}$ is the minimum energy of the incident particle when it exits the target. Then, the saturation yield (SY) which specifies the activity at saturation is given by

$$SY_{\sigma} = \frac{TY_{\sigma}}{\lambda}, \qquad (5)$$

and the target yield of measured activity of an isotope with activity A at time t_c after the end of bombardment is

$$TY_{exp} = \frac{A\lambda e^{\lambda t_c}}{I(1 - e^{-\lambda t_{irr}})},$$
(6)

where $t_{\rm c}$ and $t_{\rm irr}$ are time of cooling and irradiation respectively. Experimental saturation yield (SY_{exp}) was determined using the value of TY_{exp} calculated from Eq. (6) plugged into Eq. (5).

2.5. Estimation of uncertainties

The uncertainties of the experimentally determined activity and cross-section data have their origin in uncertainties of the detection efficiency (<4%), the statistics of counting and photo-peak area determination (<3%), nuclear data and intensities of gamma lines used (<4%), and quality of the monitoring reaction data used in the evaluation (<7%) (discussed in Sec. 3.1), uncertainty in the beam energy leading to a change in monitoring reaction (5%) and foil thickness (<1%). The total uncertainty of measured cross section and yield was obtained by adding the above-mentioned uncertainties in quadrature. Obtained total uncertainties are 11% for cross section and 8% for yield.

3. Results and discussion

3.1. Absolute normalization to $^{nat}Mo(p,x)^{m+g96}Tc$ data

The energy loss or degradation of the incident proton beam in the target was calculated using Geant4 [23] and SRIM [22] assuming incident proton energy as 26 MeV on ^{nat}Mo. The target used in the experiment is quite thick, hence average of energies within the target defines energy scale of all deduced parameters. $^{\rm nat}{\rm Mo}(p,x)^{m+g96}{\rm Tc}$ monitoring reaction [26] was used to determine the integrated beam current. Gamma lines 778.22 keV, 812.54 keV and 849.86 keV were used in data evaluation. Integrated beam current obtained from this method was 28.5 ± 3 nA.

3.2. Cross section of Tc isotopes and ⁹⁹Mo production

The determined production cross sections of 94 Tc, 95 Tc, ^{95}m Tc, 96 Tc, 99m Tc and 99 Mo radionuclides are presented in Table II and compared with the existing data in Fig. 2. Since the target used in the experiment degraded the impinging beam energy by almost 7 MeV, the resulting calculated cross section is, in fact, averaged over the energy range of 19–26 MeV. Therefore, we compared our results with the existing data averaged over the same interval of proton energy. Figure 3 (a)–(f) shows the average cross-section comparison of our results with the literature data.

TABLE II

Measured cross section of 94 Tc, 95 Tc, 95 Tc, 96 Tc, 99 mTc and 99 Mo radionuclides produced in $^{\rm nat}$ Mo averaged over the proton energy range of 19–26 MeV.

Radionuclides	Cross section [mb]
94Tc	60 ± 7
$^{95}\mathrm{Tc}$	120 ± 10
$^{95m}\mathrm{Tc}$	40 ± 5
$^{96}\mathrm{Tc}$	120 ± 10
$^{99m}\mathrm{Tc}$	110 ± 10
$^{99}\mathrm{Mo}$	110 ± 10

To calculate the cross section of 94 Tc, photo-peaks of 702.62 keV ($I_{\gamma}=99.6\%$) and 871.09 keV ($I_{\gamma}=99.9\%$) were used. 94m Tc also produces 871.09 keV ($I_{\gamma}=94\%$) gamma line, but for the reasons discussed in Sec. 2.3, its contribution can be neglected. It is evident from Fig. 3 (a) that the obtained result is in agreement with the literature data, except those from Ref. [7].

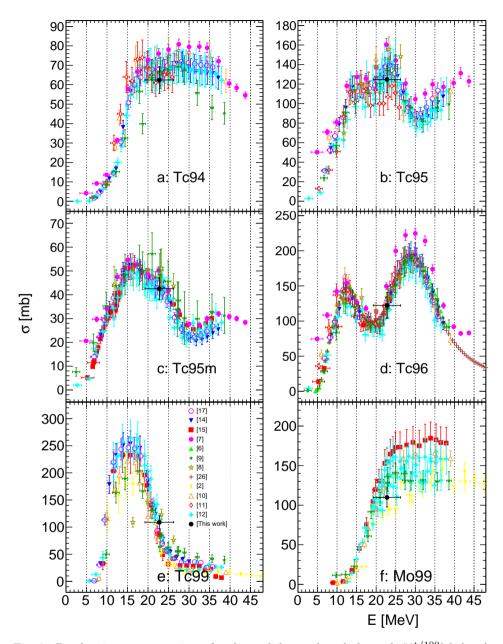


Fig. 2. Production cross section of radionuclide produced through $^{\mathrm{nat/100}}\mathrm{Mo}(p,x)$ reactions, where panels (a), (b), (c), (d), (e) and (f) represent cross sections of $^{94}\mathrm{Tc},~^{95}\mathrm{Tc},~^{95m}\mathrm{Tc},~^{99m}\mathrm{Tc}$ and $^{99}\mathrm{Mo},$ respectively. Here, the horizontal error bar represents the range of integration, not the energy uncertainty.

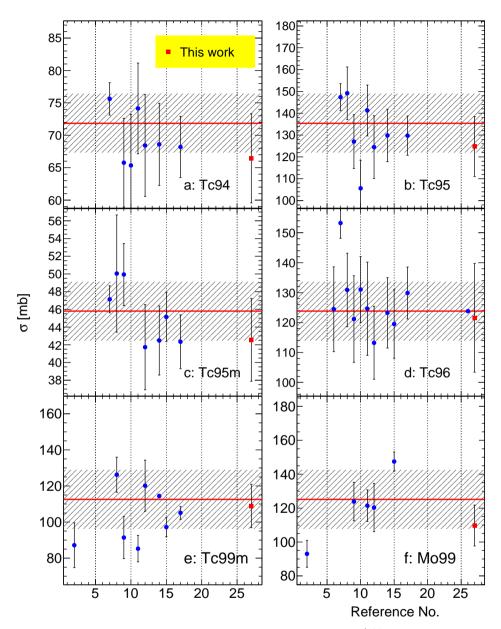


Fig. 3. Cross section of radionuclide produced through $^{\mathrm{nat/100}}\mathrm{Mo}(p,x)$ reactions averaged over the proton energy range of 19–26 MeV where panels (a), (b), (c), (d), (e) and (f), respectively, represent cross sections of $^{94}\mathrm{Tc}$, $^{95}\mathrm{Tc}$, $^{95m}\mathrm{Tc}$, $^{96}\mathrm{Tc}$, $^{99m}\mathrm{Tc}$ and $^{99}\mathrm{Mo}$. The hatched bands represent standard deviation of literature data. The labels of x-axis represents the reference numbers from the reference list.

The production cross section of 95 Tc is calculated by analyzing 765.79 keV ($I_{\gamma}=93.82\%$) gamma peak and confirmed by the analysis of the 1073.71 keV ($I_{\gamma}=3.74\%$) transition. Figure 3 (b) shows the present result for 95 Tc radioisotope. Our result is consistent within the uncertainties with most of the data points, except for those from Refs. [10] and [11].

In order to calculate production cross section of 95m Tc radioisotope, we considered the 204.11 keV ($I_{\gamma} = 63.25\%$) gamma line. Possible interference of 95m Nb ($I_{\gamma} = 2.3\%$) gamma line with the same energy was insignificant for the detectors geometry used in the measurement. For the production of this radioisotope the obtained cross section agrees with the literature data (shown in Fig. 3 (c)).

 96m Tc ($T_{1/2}=51$ min) is a short-lived radioisomer of 96 Tc ($T_{1/2}=4.28$ days). 98% of 96m Tc decays to 96 Tc by the internal conversion process and emits very weak gamma spectral lines that are not suitable for quantitative study [8]. Although this isomer can also feed the 778.22 keV spectral line of 96 Tc, its contribution can be neglected due to a large ratio of cooling time to its half-life. For the production cross section of 96 Tc, we considered 778.22 keV ($I_{\gamma}=99.9\%$) line and the results were cross-checked with 812.58 keV ($I_{\gamma}=82.4\%$) transition, determined cross-section values from both photo-peaks were consistent. Figure 3 (d) shows the comparison of present data with other data available in the database. Our data is in good agreement with all other reported data except results from [7].

As discussed in Sec. 2.3, we used the 140.51 keV spectral line to calculate production cross section of 99m Tc and 99 Mo. Reported cross sections are not cumulative. They were calculated separately for 99 Mo and 99m Tc after suitable correction in the activation formula. For determination of 99 Mo production cross section, we used data collected after at least 77 hours of cooling time, which justifies the neglect of contribution from directly produced 99m Tc. Average cross section of 100 Mo $(p,x)^{99m}$ Tc compared with other existing data is shown in Fig. 3 (e). Within the error bars, our result is in good agreement with other data points except those from Ref. [11], which are slightly lower. Figure 3 (f) shows the averaged cross-section comparison of 100 Mo $(p,x)^{99}$ Mo, our result is consistent with other data points within the error limits, only the data point from Ref. [15] deviates upwards from the trend.

3.3. Target yield and saturation yield

Directly determined integral target yields of all studied radionuclides are presented in Table III. Integral target yield was calculated using Eq. (6). Target yield is expressed in MBq/ μ Ah (*i.e.* for 1 hour of irradiation at 1 μ A beam current). The obtained results are shown in Fig. 4 as a function of

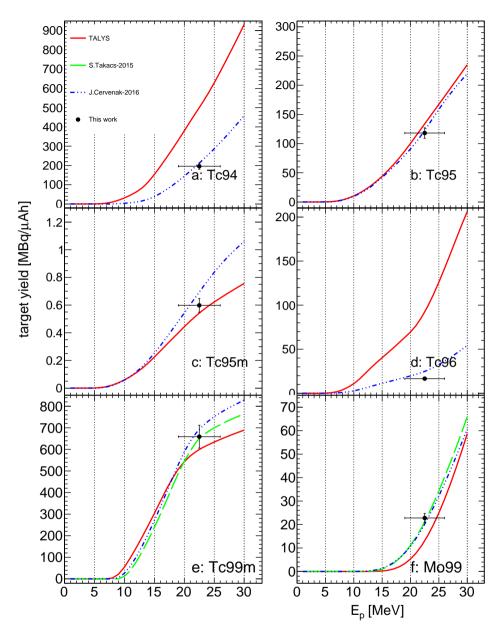


Fig. 4. (Color online) Integral TY of $^{\rm nat}{\rm Mo}(p,x)$ reaction; here, long dashed/green and dash-dotted/blue curves represent the experimental TY from [15] and [17], respectively, and the solid/red curve is from TALYS. Here, the error bar represents the range of integration not the energy uncertainties.

TY and SY of 94 Tc, 95 Tc, 95 mTc, 96 Tc, 99m Tc and 99 Mo radionuclides produced by proton irradiation on $^{\rm nat}$ Mo target.

-		
Isotope	TY [MBq/ μ Ah]	SY [MBq/ μ A]
⁹⁴ Tc	200 ± 20	1380 ± 110
$^{95}\mathrm{Tc}$	120 ± 10	3410 ± 270
$^{95m}\mathrm{Tc}$	0.60 ± 0.05	1290 ± 100
$^{96}\mathrm{Tc}$	20 ± 1	2560 ± 200
$^{99m}\mathrm{Tc}$	660 ± 50	5710 ± 460
$^{99}\mathrm{Mo}$	20 ± 1	2190 ± 170

incident proton energy and are compared with TY from [17] and TALYS [27] predictions. In the case of ⁹⁹Mo and ^{99m}Tc, we have compared the results also with data from Ref. [15]. TY from [15] and [17] were calculated using the fitted experimental data (cross-section data was used from [28]) and stopping power of protons in molybdenum in the measured energy range. Similarly, TY from TALYS was calculated using cross-section data from TALYS.

As seen in Fig. 4, integral TY data is in good agreement with [17] and [15] within the error limits. In the case of $^{\rm nat}{\rm Mo}(p,x)^{94,96}{\rm Tc}$, TALYS predictions are higher than the experimental data, in other cases, TALYS predictions are in agreement with experimental TY.

4. Conclusions

We measured the average cross section for the production of 94 Tc, ^{95}m Tc, 96 Tc, ^{99}m Tc and 99 Mo radionuclides through nat Mo(p,x) reactions in the proton energy range of 19–26 MeV. The determined cross sections have been compared to existing data and they show consistency with most of them. The target yields were deduced from the measured activity of all listed radioisotopes. Target yields determined in the experiment have been confronted with the results of [15, 17, 27]. TALYS target yield predictions are found to be not in agreement with this experimental values in the case of nat Mo $(p,x)^{94,96}$ Tc.

Currently, the price of enriched Mo is about \$30,000 per gram, whereas for $^{\rm nat}$ Mo the price varies from \$0.25 to \$0.80 per gram [29]. By using natural molybdenum targets, one can reduce the cost and meet the desired yield by increasing the irradiation time. Using protons of energies of 9–26 MeV will help to reduce the production of impurities. It was demonstrated that use of $^{\rm nat}$ Mo target could provide a very pure 99 Mo source for extraction of 99m Tc with standard methods [7, 30].

As our results agree with other available data, the presented experiment and its results prove that the experimental setup is well-understood, with this data analysis procedure we will go for a measurements at lower energy, with stack-foil activation method.

This work was supported by the DSC 2017 grant intended to finance the development of young researchers and Ph.D. students of the Faculty of Physics, Astronomy and Applied Computer Science with the decision number MNSW: 7150/E-338/M/2017. The authors are thankful to the staff of AIC-144 cyclotron for the excellent work.

REFERENCES

- [1] T.J. Ruth, La Physique AU Canada 66, 15 (2010).
- [2] B. Scholten et al., Appl. Radiat. Isot. **51**, 69 (1999).
- [3] M.C. Lagunas-Solar et al., Int. J. Radiat. Appl. Instrum. A 42, 643 (1991).
- [4] National Research Council, Medical Isotope Production Without Highly Enriched Uranium, The National Academies Press, Washington, DC, 2009.
- [5] S. Takács et al., J. Radioanal. Nucl. Chem. 257, 195 (2003).
- [6] S. Takács, F. Tárkányi, M. Sonck, A. Hermanne, Nucl. Instrum. Methods Phys. Res. B 198, 183 (2002).
- [7] M. Bonardi, C. Birattari, F. Groppi, E. Sabbioni, Appl. Radiat. Isot. 57, 617 (2002).
- [8] M.U. Khandaker et al., J. Korean Phys. Soc. 48, 821 (2006).
- [9] M.U. Khandaker et al., Nucl. Instrum. Methods Phys. Res. B 262, 171 (2007).
- [10] A.A. Alharbi, J. Alzahrani, A. Azzam, *Radiochim. Acta* **99**, 763 (2011).
- [11] A.A. Alharbi et al., Medical Radioisotopes Production: A Comprehensive Cross-section Study for the Production of Mo and Tc Radioisotopes via Proton Induced Nuclear Reactions on nat Mo, in: Radioisotopes — Applications in Bio-Medical Science, Prof. N. Singh (Ed.), pages 3–26, 2011.
- [12] F. Tárkányi et al., Nucl. Instrum. Methods Phys. Res. B 280, 45 (2012).
- [13] P. Chodash et al., Appl. Radiat. Isot. 69, 1447 (2011).
- [14] O. Lebeda, M. Pruszyński, *Appl. Radiat. Isot.* **68**, 2355 (2010).
- [15] S. Takács et al., Nucl. Instrum. Methods Phys. Res. B **347**, 26 (2015).
- [16] F. Tárkányi et al., J. Radioanal. Nucl. Chem. 319, 487 (2019).
- [17] J. Červenák, O. Lebeda, Nucl. Instrum. Methods Phys. Res. B 380, 32 (2016).
- [18] S.M. Qaim et al., Appl. Radiat. Isot. 85, 101 (2014).
- [19] K. Szkliniarz et al., Mod. Phys. Lett. A 32, 1740012 (2017).
- [20] S.M. Qaim, Nucl. Med. Biol. 44, 31 (2017).

- [21] J. Meija et al., Pure Appl. Chem. 88, 293 (2016).
- [22] J.F. Ziegler, J.P. Biersack, M.D. Ziegler, SRIM code, version 2013.
- [23] Geant4 (simulation software), version 10.2.3, 2017.
- [24] Nuclear structure and decay data.
- [25] M.S. Uddin et al., Appl. Radiat. Isot. 60, 911 (2004).
- [26] A. Hermanne et al., Nuclear Data Sheets 148, 338 (2018).
- [27] TALYS (software), version 1.9, 2018.
- [28] Experimental Nuclear Reaction Data (EXFOR), 2018, database version of November 29, 2018.
- [29] T. Michael Martin et al., J. Radioanal. Nucl. Chem. 314, 1051 (2017).
- [30] M. Gumiela, J. Dudek, A. Bilewicz, J. Radioanal. Nucl. Chem. 310, 1061 (2016).